FAILURE MODE ESTIMATION AT HIGHLY LOADED THICK COMPOSITE LUGS REPRESENTING ROTARY WING UAS BLADE ROOT

Gokhan Tursun, Betul Pelin Maradit, Evren Eyup Taskinoglu

Turkish Aerospace Industries, Inc. (TAI),
Integrated Helicopter Systems
ODTU Teknokent A-Blok 06531, Ankara, Turkey

gtursun@tai.com.tr (Gokhan Tursun)

ABSTRACT

Tendency to use thick composites in primary aerospace structural applications has increased recently. Not only the accurate modeling of the mechanical and failure behavior of the thick laminates but also the manufacturing and process quality assurance of these heterogeneous structures is crucial in order to obtain acceptable products. Manufacturing process should be resolved during the design and failure types must be investigated during the analyses. In addition, detailed considerations are necessary for small Rotary Wing Unmanned Aerial Systems (RW-UAS) in terms of structural design, manufacturing processes and dynamic characteristics due to their high RPM requirements and difference in scale.

In the scope of this study, thick composite lugs representing the small RW-UAS main rotor blade root are designed and analyzed; considerations about testing of the prototypes are given. Since the root section of the main rotor blade attaching the blade to the hub exposed to very high and complex loads, special attention is given to the design of this region. Both carbon fiber reinforced polymers (CFRP) and glass fiber reinforced polymers (GFRP) lugs including also metal bushings for the connection to the hub are designed. Specifying the loads exerted to the blade root, a detailed finite element analysis (FEA) including progressive failure study is carried out. Several alternative analysis methods are evaluated under reliability and practicality considerations. As the analysis with plane stress shell elements does not give accurate results, 3D FEA defining all material properties and ply orientations is performed for thick composite blade root. Dynamic characterization of the blade root is performed and evaluated under high RPM requirements. Design variable sensitivities are investigated by evaluating the cost, stock and manufacturing constraints. Some test specimens representing the thick laminates are manufactured subsequently several static and fatigue tests are conducted. Due to the complexity in determination of the composite rotor blade fatigue characteristics, a representative service-life simulation fatigue test has been performed on scaled test specimens by applying the realistic loads identified as in-service loads. As a

fatigue test outcome, obtained service life of the rotor blade is evaluated in terms of safe-life requirements.

The test results which expand the understanding regarding thick laminates are essential and valuable source to the validation of the FEA results and 3D failure mode estimation. Model-test correlation is used as a tool for determining the deltas between the actual design and the manufactured rotor blade. The observed differences are highlighted in order to be used in manufacturing quality assessment and improvement. Moreover non-destructive tests are performed in order to verify the manufacturing quality and process control of thick laminates. Non-destructive test results are analyzed in terms of static and fatigue criteria's and life extension capability of the fatigue tested rotor blade is investigated. The assurance of the compatibility of the design, manufacturing and test phases of the lugs representing helicopter main rotor blade root is planned in the light of the "Building Block Approach" principles.

1. INTRODUCTION

It has long been recognized that the classical two-dimensional laminated plate theory, based on the Kirchhoff hypothesis of straight inextensional normals for the entire plate package yields sufficiently accurate results only for thin composite plates [1, 3]. For three dimensional (3D) analyses of laminates, plane stress shell elements do not give reasonable results, thus another numerical or analytical methods should be investigated for thick laminates. Most of the advanced composites in use to date have a low ratio of the transverse shear modulus to the in-plane modulus, and therefore the transverse shear deformation plays a much more important role in reducing the effective flexural stiffness of laminated plates made of these composites than in the corresponding metallic plates [2]. The transverse shear deformation was found to be important in predicting the delamination type of failure in multilayered composite structures [5]. Furthermore there are several parameters affecting the design and manufacturing of the composites. In order to get an effective outcome, composite materials are to be designed, manufactured and tested properly as well as consistently. For composite structures, the deficiencies in the design, manufacturing and testing or incompatibilities between these phases may cause dramatic consequences such as delamination, matrix failure, fiber break and interface debonding in the service. Therefore, "Building Block Approach" principles which assure all these phases' reliability should be considered during composite design [1].

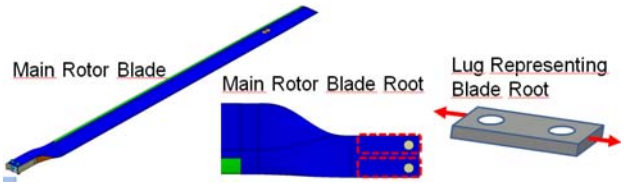

Figure 1: An example of Rotary Wing UAS main rotor blade and its root section: component (main rotor blade), sub-component (root section), detail (lug)

In this work, thick composite lugs representing the helicopter main rotor blade root are designed, analyzed, manufactured as well as tested (see Figure 1). Mostly there are three alternatives in designing the composite blade root. The first method is to wrap the fibers around metallic or composite bushing, the second way is the flexbeam concept and the third technique is to drill the thick composite root section in order to provide holes for blade-hub connection. Within this study the details of last method

is focused on due to the manufacturing constraints and it is intended to obtain understanding on the strength and failure behavior of the drilled thick composite lug.

Basically three fundamental failure behaviors are observed in the lugs: net-tension, shear-out, and bearing [2]. In net-tension failure, matrix and fiber tension failure due to stress concentrations are dominant whereas in bearing and shear-out failures occur mainly because of the shear and compression failures of fiber and matrix [7, 8]. In this study, first of all several test specimens of CFRP and GFRP lugs with different stacking sequences are manufactured. The manufacturing and process quality of the specimens are controlled with non-destructive inspections.. The static tension tests for lug specimens are performed. Subsequently finite element analysis (FEA) results are compared with test results. An appropriate three dimensional (3-D) analysis method is investigated in the light of the test results. MSC. Marc which has a suitable element type for 3-D composites is used in FEA. Due to the wide range of the test results, merely CFRP lug test and analysis results are concentrated and presented in the following sections.

2. MANUFACTURING

The manufacturing and process controls are extremely crucial for laminated structures. In order to get an appropriate composite structure, compatible with designed ones, all the steps followed in manufacturing should be observed cautiously. In this study CFRP and GFRP thick lug specimens whose thicknesses vary between 15-20 mm are manufactured by hand lay-up. In Figure 2, samples of thick composite lugs are shown. Before mechanical testing of the composite lugs, non-destructive test (NDT) is carried out for all specimens and the manufacturing and process quality assurance is obtained [12].

(a)

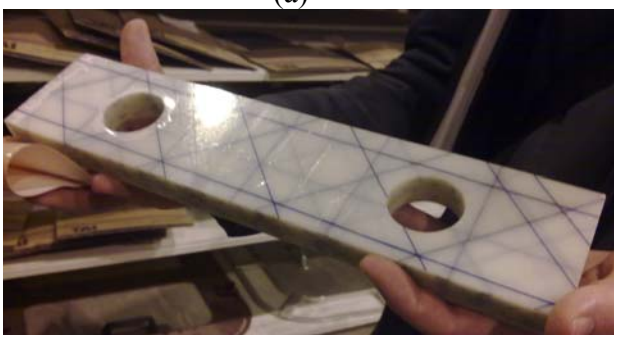

(b)

Figure 2: Manufactured (a) CFRP and (b) GFRP lugs

However some troubles during machining and bushing installation of thick composite lugs are encountered. Machining of the composites is an issue that should be evaluated separately and deeply. After manufacturing of composite lug specimens, they are machined in the light of given test specimen dimensions. Particularly, during the drilling operation of the thick laminate, several details influence on the quality of the hole such as drilling machine sensitivities, cutter material properties, cutter angle and speed as well as the laminate material properties (thickness, stacking sequence, etc.). Moreover, bushing installation into a thick composite lug is also significant [11].

For instance in the beginning of specimen manufacturing phase, some problems are recognized regarding these issues. In Figure 3 (a), CFRP lug specimen after freeze fitted steel bushing, delamination in the vicinity of the hole is detected with NDT. On the other hand, before installing a bushing to the lug, to drill a hole into GFRP lug is itself very challenging. Delamination which is observed during drilling operation is demonstrated in Figure 3 (b). These specimens are listed as scraps and by means of some improvements for machining and bushing installation, such obstacles are solved.

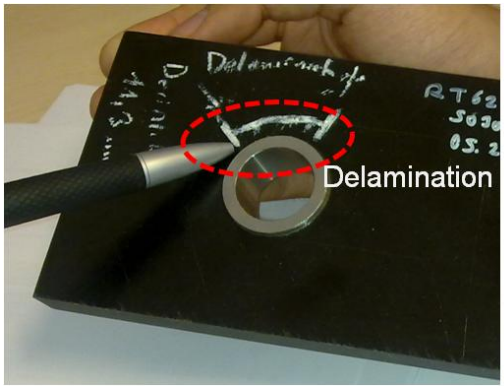

(a)

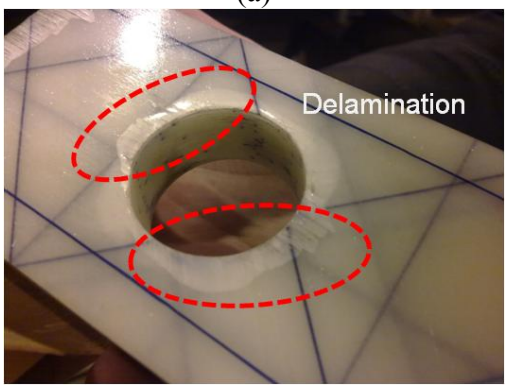

(b)

Figure 3: Delaminations around the hole in thick laminates a) due to metal bushing installation in CFRP lug, detected by NDT b) due to hole drilling into GFRP lug, detected by eye-inspection

3. EXPERIMENTS

3.1 Instrumentation of CFRP Lug

After validating manufacturing quality of the test specimens, they are instrumented with strain gauges and rosettes for static tension test preparation. For each configuration three specimens are manufactured and tested, thus three CFRP lug specimens are instrumented and prepared for test individually. The CFRP lug is instrumented with ten strain gauges (SG) and with two strain rosettes (SR). Two strain gauges around each hole (SG1,2,9,10), three strain gauges in the middle section (SG3,5,6) of the lug, one strain gauge on the other side of mid section (SG4), two strain gauges on the thickness direction of the lug (SG7,8) and two strain rosettes (SR1,2) around each hole are considered. The location of the strain gauges and rosettes is illustrated in Figure 4.

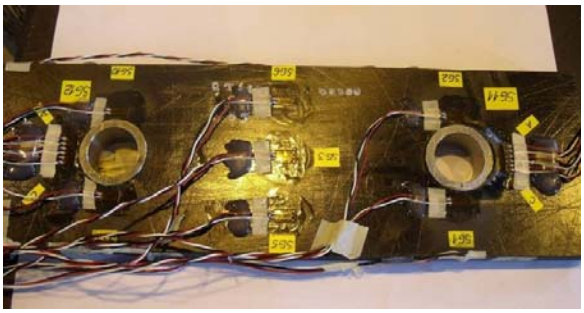

Figure 4: Instrumentation of the CFRP lug specimen with strain gages

3.2 Static Tension Test Set-up

The static tension test is conducted with MTS test system which has a 2500 kN capacity. The tension test is a displacement controlled test via test speed 0.05 mm/min. In Figure 5, test-set up for tension static test of the 15mm thick CFRP lug is shown.

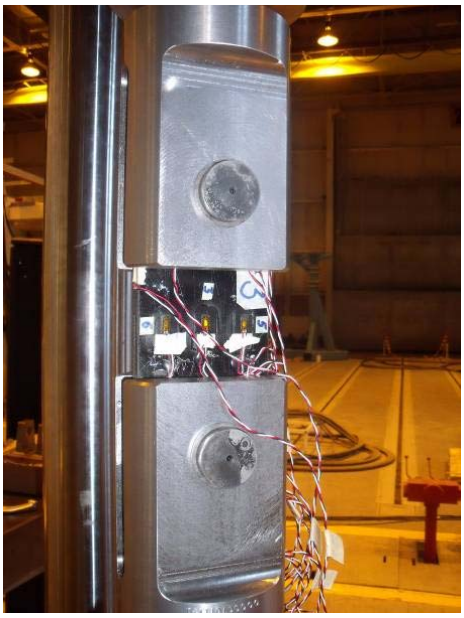

Figure 5: Test set-up for static tension test of CFRP lug

3.3 Fatigue Test

It is crucial to validate a new blade design by considering the operational service usage on a realistic fatigue test. The objective of a fatigue test is, from a designer's point of view, to determine the fatigue life of a test piece, a specimen, or a component, subjected to prescribed sequences of stress cycles so as to predict the fatigue life in actual service [15].

Service spectrum plays a major role in life determination of any structural component. Determination of service spectrum is a challenging task when we think of the variability of the loads in service especially for helicopter blades. It is essential to determine the origin of the fluctuating loads on the blade surface in order to develop fatigue spectrum to be used in analysis and tests. Centrifugal loading and bending moment due to dynamic loading gradually increase towards the root portion of the blade and reach their maximum value at the blade root.

In the current fatigue test, only the blade fatigue characteristic due to axial loading is investigated. Due to current test set-up limitation, coupling the aerodynamic loading with centrifugal loading is not possible. The aim in performing this test is to investigate the fatigue strength of the helicopter blade by comparing the root stress gradients simulated in test with the stress distributions obtained from FE by the application of centrifugal and aerodynamic loading. However, this can only provide polemic clues about the fatigue behavior of the helicopter blade due to absence of the loading physics not simulated in the current fatigue test.

Thus, a further fatigue test is planned to clarify the blades fatigue characteristics. In the planned fatigue test, the centrifugal and aerodynamic load, mimicking the actual loading expected in service, will be applied simultaneously.

The current fatigue tests are performed by using the static test setup and aiming to find the fatigue limit of the blade based on axial loading. For this purpose, three test specimens will be used and the test loading will be updated according to the cycles achieved in the prior fatigue tests.

The initial fatigue test is conducted by using the %70 of the centrifugal load. Based on the number of cycles achieved in this test, the loading on the blade will be increased or decreased to achieve a number of cycles around 5x106. The reason of this target is to prevent over-conservativeness in fatigue curve due to test results obtained below fatigue limit (number of cycles above 10^7).
The test loading and the strain gauge measurements are monitored during the fatigue test in order to verify the load applied and to anticipate possible internal failure mechanisms. The strain gauge

measurements at $2.25x10^6$ shows consistent trend that can be used to conclude intact behavior of the tested structure.

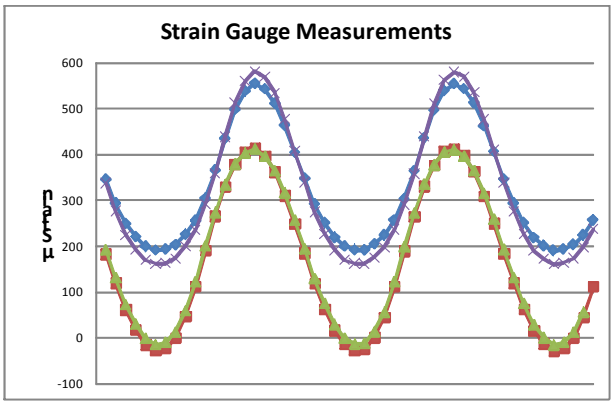

Figure 6: Strain Gauge Measurements around 2.25x106 Test Cycles

3.4 Non-destructive Testing

In order to evaluate the composite blade design in terms of structural integrity aspects, determination of the damage mechanisms associated with the structure is required. Thus, suitable means of inspection methods should be defined for the structure in use or in test. To investigate the general damage characterization of the structure, for example damage growth under cyclic loading, it is necessary to prevent degradation of the structure for inspection purposes. Hence non-destructive testing methods are favorable when we think of the available amount of information that can be gained by examining the blade in service/test.

Non-destructive testing (NDT) involves the use of noninvasive measurement techniques to gain information about defects and various properties of materials, components, and structures needed to determine their ability to perform their intended function and prevent failure [16]. There are several numbers of Non-destructive testing techniques such as Visual Inspection, Magnetic Particle, Liquid Penetrant, Radiography, Ultrasonic NDT, Eddy Current, Tap Test, Thermography etc. Unfortunately, the application of these techniques on composites is limited when we think of the complex nature of the composite structures, especially for turbine blades. Turbine blades are complicated objects for inspection by non-destructive techniques: they are multilayered, have a variable thickness, have an arbitrary curved surface, are made from anisotropic materials and have a lot of manufacturing non-homogeneities.[17].

General NDT techniques used in composite materials are Visual Inspection, Ultrasonic NDT, Tap Test, Radiography and Thermography. These techniques have different capabilities in determination of defects such as delamination, debonding, porosity, impact damage etc. Composite defects that can be detected by the various NDT techniques are listed in the below table [18];

	NDT Technique						
Defect Type	Ultrasonics	Radiography	Eddy Current	Acoustic Emission	Thermography	Optical Holography	Mechanical Impedance
Voids, porosity	Yes	Yes			Some	Some	Some
Debonds	Yes	Some		Some	Yes	Yes	Yes
Delaminations	Yes	Some		Some	Yes	Yes	Yes
Impact damage	Yes	Yes	Yes		Some	Some	Some
Resin variations	Yes	Some					
Broken fibers	Yes	Some	Yes	Yes			
Fiber misalligment	Yes	Yes	Yes				
Resin cracks	Yes	Some					
Cure variations	Yes				Yes	Yes	Yes
Inclusions	Yes	Yes					
Moisture	Yes						

Table 1: Applicable composite NDT techniques

So applicability of the employed inspection technique should be questioned during investigation of a certain type of defect. Ultrasonic inspection is the most often used non-destructive composite testing method in the industry and it is reliable and efficient

while having the capability of quick determination of flaws. [18]. Fundamentally a probe with a piezoelectric crystal transmits ultrasonic pulses into the specimen and whenever a change in material acoustic impedance occurs the pulses are reflected back and received by the same or another crystal [19].

The detailed non-destructive inspections of the fatigue tested specimens are planned in order to assess the failure mechanism and possible life extension capability of the structure. Current planned/available inspection methods are Ultrasonic NDT and Radiography.

4. NUMERICAL PROCEDURE

Simulations are performed by using commercial FEA software MSC.Marc® with contact and boundary conditions that are based on the experimental study. Composite material is modeled by using a 3D, eight node composite brick element in which each composite layer has four integration points (see Figure 7).

This element type is suitable for 3D composite analysis [13, 14]. Two rigid bodies are established in order to model bolts. One of the pins is immobile whereas the other has a constant velocity of 0.05mm/min. Both of the bushings are perfectly bonded with the test body and they are in contact with the pins. After successive refinement of mesh, it is observed that 1720 elements produce stable and safe results.

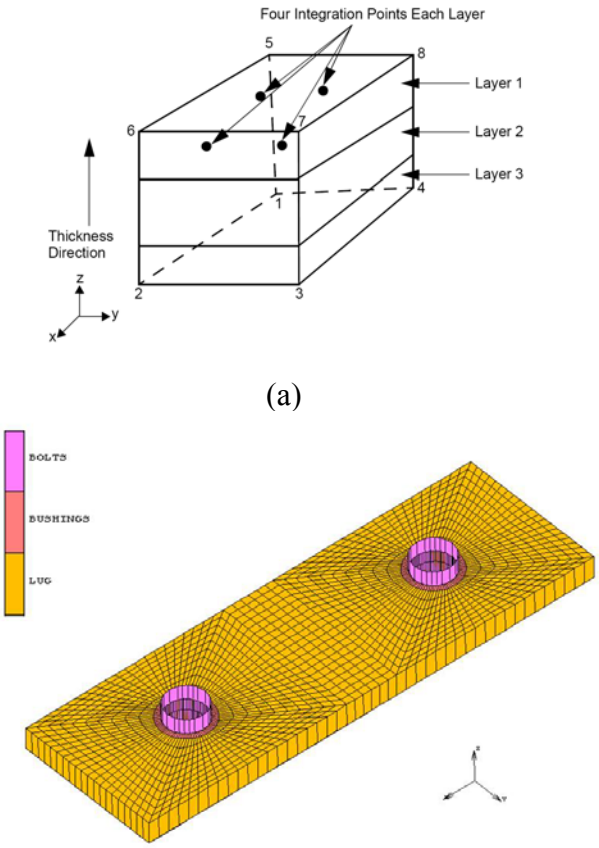

Figure 7: FEA details; a) Typical 8-node 3-D composite element, element type 149 in MSC.Marc b) 3D finite element model of the composite lug

Normally the root section of the main rotor blade exposed to very high and complex combined tension, bending, torsion loads. However, in this study in order to understand failure behavior of thick composite lug under centrifugal load, only tension load case is taken into account.

Furthermore, to estimate failure behavior of the thick composite lug, different failure theories are applied during FEA. Laminated composites failure criteria may be classified into three groups: non-interactive theories (maximum stress, maximum strain); interactive theories (Tsai-Hill, Tsai-Wu); and partially interactive or failure mode-

based theories (Puck). Maximum Stress, Tsai-Wu, Hashin, Puck and Hoffman failure criteria are studied [10]. After evaluating the test data a proper failure criteria for thick composite lug is investigated.

CFRP – UD Material Properties	
Thickness: 0,185 mm	**Xt/Xt :** 1
E1/E1 : 1	**Xc/Xt :** 0,783
E2/E1 : 0,054	**Yt/Xt :** 0,016
E3/E1 : 0,054	**Yc/Xt :** 0,105
G12/E1 : 0,025	**Zt/Xt :** 0,016
G23/E1 : 0,020	**Zc/Xt :** 0,105
G31/E1 : 0,025	**Sxy/Xt :** 0,064
Nu12/Nu12 : 1	**Syz/Xt :** 0,059
Nu23/Nu12 : 0,6	**Szx/Xt :** 0,059
Nu31/Nu12 : 0,02	

Table 2: Material data for CFRP UD layers

CFRP – UD Material Properties	
Thickness: 0,185 mm	**Xt/Xt :** 1
E1/E1 : 1	**Xc/Xt :** 0,783
E2/E1 : 0,054	**Yt/Xt :** 0,016
E3/E1 : 0,054	**Yc/Xt :** 0,105
G12/E1 : 0,025	**Zt/Xt :** 0,016
G23/E1 : 0,020	**Zc/Xt :** 0,105
G31/E1 : 0,025	**Sxy/Xt :** 0,064
Nu12/Nu12 : 1	**Syz/Xt :** 0,059
Nu23/Nu12 : 0,6	**Szx/Xt :** 0,059
Nu31/Nu12 : 0,02	

Table 3: Material data for CFRP Fabric layers

For CFRP lug, the combination of uni-directional (UD) and fabric layers are considered in stacking sequence configuration so as to get optimum load-bearing lug. The number of the fabric (+/-45^0) layers and UD (0^0) layers utilized in the lug is almost equal. The material properties and allowables of CFRP UD and fabric layers are determined with numerous coupon tests and these values are used in the FEA analysis (see Table 1 and 2).

After performing the simulations, strain data is extracted from the nodes that are located close to the strain gauge positions that are illustrated in Figure 4.

5. RESULTS

5.1 Experimental Results

As mentioned earlier, three CFRP lug specimens for same configuration are manufactured and tension test is executed for each of them. In Figure 8, test results of four strain gauges (SG) are presented. It is clear from the figure that tests are quite repeatable. SG1- SG10 and SG3-SG4 couples give consistent results.

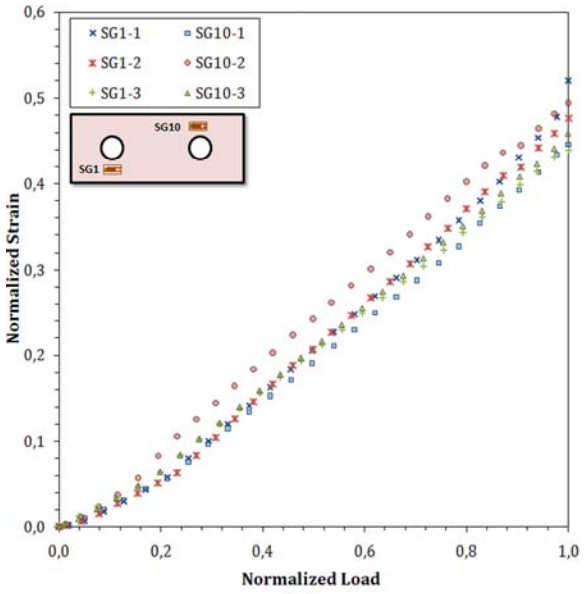

(a)

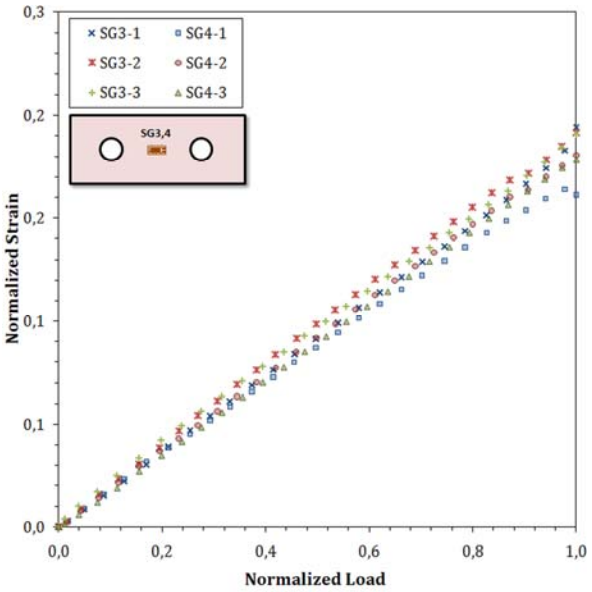

(b)

Figure 8: Test results at strain gauge positions (a) SG1 and SG10 results (b) SG3 and SG4 results (here "-1, -2 and -3" stands for the test numbers, e.g. SG1-1 refers first strain gauge result of first test).

The consistency of SG3-SG4 (located at front and back side of the lug) shows that specimen is well-aligned and there is no undesirable bending in the test (see Figure 8 (b)).

All of the strain results obtained from third test are shown in Figure 9. Strains at the right and left hand side of the holes and at the centerline of the test specimen are positive (tensile) whereas, the ones that are located close to the edge are negative (compressive). At the end of the test failure occurred at the region where strains are negative (see Figure 10); in fact, the instant of failure can clearly be seen from the corresponding curves (SR1A-B-C and SR2A-B-C).

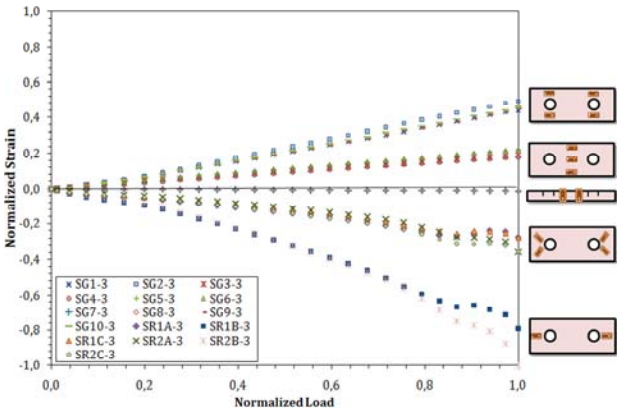

Figure 9: Test results; Load-Strain curves at different strain gauge and rosette positions (here "SG" refers "strain gauge", "SR" refers strain rosette, whereas "-3" stands for "3rd test")

The tension test controlled by displacement is carried on until total failure. In Figure 10, it can be clearly observed that bearing failure occurred in the end of the test in CFRP lug which is fail-safe designed [6] (w=3D, e=2D, where w: width of the lug, D: hole diameter, e: edge distance)

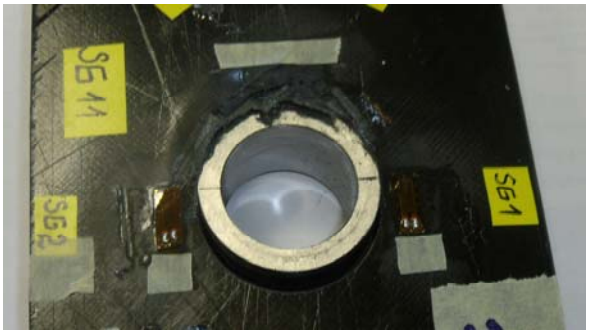

Figure 10: Bearing failure observed in CFRP lug

5.2 Simulation Results

In this study, failure mode of CFRP lugs by using an optimum and representative FEA model is investigated. To do this, aforementioned tests are modeled by simple linear elastic analysis with displacement controlled pins and perfectly bonded bushings. Subsequently model is

successively modified to obtain most experimentally consistent results. The modifications are made on progressive failure and failure criteria.

In the first model; a simple linear elastic analysis is performed. Experimentally measured longitudinal strains at the most critical locations; namely, hole neighborhood, and simulation results (referred as "*simulation*") are compared in Figure 11. These results indicate that experiment and simulation coincide at the very beginning of the test, but later simulation results significantly deviate. As load increases, model behaves much more stiff then actuality. This might be owed to the gradual decrease in stiffness due to local failure that is brought in to material during the test. In order to model this effect; progressive failure analysis is performed. Material is assumed to be linear elastic until failure. At failed elements, moduli are degraded with a factor based on utilized failure index (FI). Gradual degradation of moduli continues until FI's drop less than or equal to one.

The application of progressive failure and its success significantly depend on the choice of failure criterion [9]. In this study, a widely used failure criterion; Tsai-Wu is used. Tsai-Wu is a polynomial failure criterion which is expressed in terms of strength parameters, and interaction coefficients. Interaction coefficients (IC) are empirically determined and they are highly sensitive to experimental errors. Moreover, it is very hard to determine in-plane and out-of plane interaction terms $F_{xy,}$ F_{yz} and F_{zx}. In most cases, interaction parameters remain with high uncertainties. Since success of the model depends on the Tsai-Wu parameters, it is important to understand sensitivity of simulation results on interaction coefficients. Therefore; during the study, not only the effect of mentioned progressive failure algorithm but also the effects of second order interaction terms are investigated by varying IC's.

Two cases of IC's are investigated;

(1) IC's=0

(2) $F_{xy}= -1/2(1/X_TX_C.\ 1/\ Y_TY_C)^{½}$
$F_{yz}= -1/2(1/Y_TY_C.\ 1/\ Z_TZ_C)^{½}$
$F_{zx}= -1/2(1/Z_TZ_C.\ 1/\ Z_TZ_C)^{½}$ where X_T, X_C, Y_T, Y_C, Z_T and Z_C are tensile and compressive strengths in x, y and z axes.

Results of these two cases are illustrated in Figure 10. Case (1) referred as "Simulation Progressive Failure, IC's=0" and case (2) referred as "Simulation Progressive Failure, IC's≠0". Interaction coefficients do not have any significant effect on strains at the initial stage of the test: before local failure starts. As anticipated, two models (1) and (2) are equivalent before failure starts. Moreover; IC's do not have much effect on the instant when first failure occurs. This might be due to the low magnitude of loading and hence quadratic terms in Tsai-Wu failure criterion.

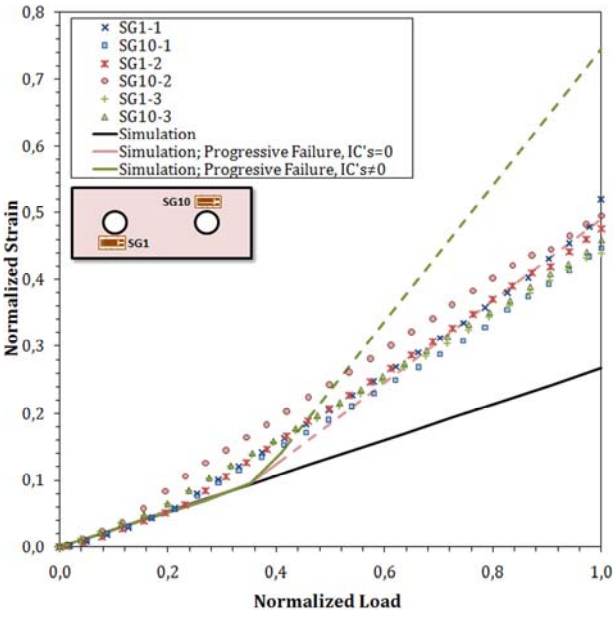

Figure 11: Comparison of experimental and simulation results.

The contour plots of Tsai-Wu failure indices for first-ply failure (at t=15min) and total failure (at t=55min.). Contour at t=15min shows (Figure 12) “first ply failure” which occur near holes, whereas; contour at t=55min shows the final state of failure indices.

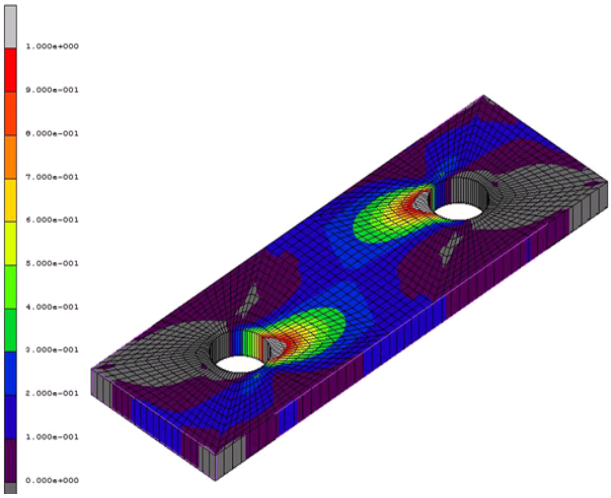

Figure 12: Contour plot showing distribution of Tsai-Wu failure indices at 1st composite layer. (a) first ply failure at t=15min

Also, Tsai-Wu indices that are extracted from nodes near strain gauge positions and at “first failure” location are presented in Figure 13. It is clear from figures that first failure occurs at 15th minute when a sharp brake observed in normalized load vs. normalized strain curves (Figure 11). At this point, case (1) and case (2) differentiate due to the differences in the extent of failure. As loading increases effect of interaction coefficients become more and more pronounced. This is owed to the increase in the magnitudes of quadratic terms and, therefore; distinction in the extent of failure. These results indicate that, implementing progressive failure into the model considerably changes strain behavior after failure. Its effect gradually increases with loading condition.

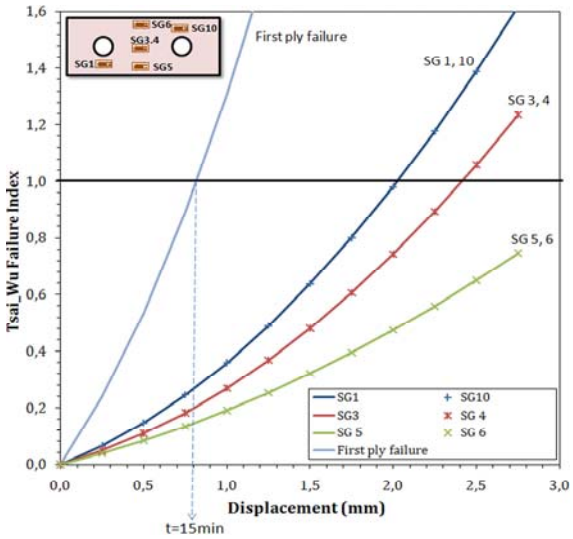

Figure 13: Tsai Wu indices extracted from nodes that are located at strain gauge positions. (IC≠0)

In summary, it is seen that finite element model qualitatively represents actual behavior of the composite lug and the prediction of failure mode is much more reasonable with progressive failure analysis. However, there are still quantitative deviations such as stiffness of the model and the failure initiation time. The following issues might be responsible for such variations;

Material and failure model is very sensitive to input data error; namely; material properties and allowable.

Selective gradual degradation method has some weaknesses in representing stiffness degradation of the modeled material,

Tsai-Wu misrepresents the failure of current 3D lamina system,

6. CONCLUSIONS

In this study by the help of the conducted static tests and finite element analysis, an understanding for prediction strength and

failure behavior of the highly loaded thick composite lugs is obtained. Furthermore the challenges of thick composite manufacturing investigated and quality assurance is provided with non-destructive tests. Machining of thick laminates, drilling an acceptable hole are another key studies performed in this work.

Having acceptable test specimens, tension tests are conducted to determine failure behavior and later a model is developed to obtain consistent results with experiments. Effect of progressive failure in combination with Tsai-Wu on quality of the results is investigated. Furthermore, sensitivity of simulation results on hard-to-determine interaction coefficients is investigated.

Finally, results show that;

Including progressive failure to the model significantly enhances the quality of the strain results,

When Tsai-Wu failure criterion is used in progressive failure model, simulation results are highly sensitive to interaction coefficients.

At low loads interaction terms has no influence on results whereas, their effects become more pronounced at higher loads.

In this study; different failure criteria such as Maximum Stress, Hashin, Puck and Hoffman are investigated to determine optimum model that represents composite thick lugs. However it is realized that developing a thick composite failure criterion based on test results is more practical. GFRP and hybrid lug configurations' static tests and detailed finite element analyses are also planned in future works.

7. REFERENCES

1. "Composite Materials Handbook, Volume 1 Polymer Matrix Composites Guidelines for Characterization of Structural Materials", MIL-HDBK-17-1F, Department of Defense Handbook, 17 June 2002

2. Bruhn, E. F. *Analysis and Design of Flight Vehicle Structures.* Jacobs Publishing, Indianapolis, IN, Chap. D1.11, 1973

3. Niu M. C. Y. *Composite Airframe Structures.* Technical Book Company, Los Angeles, 1996

4. Reddy D.J. "Composites in Rotorcraft Industry & Damage Tolerance Requirements." *FAA Composites Workshop*, 2006.

5. Kuhlmann G., Rolfes R. "A Hierarchic 3D Finite Element for Laminated Composites." *International Journal for Numerical Methods in Engineering*, Volume 61, Issue 1, pages 96–116, 7 September 2004

6. Wallin M., Saarela O. and Pento F. "Load Response And Failure Of Thick RTM Composite Lugs." *ICAS2002 Congress.* 314.1-314.9, 2002

7. Kassapoglou C., Townsend Jr. W. A. "Failure Prediction of Composite Lugs Under Axial Loads." *AIAA Journal.* Vol. 41, No. 11, November 2003

8. Havar T. and Stuible E. "Design And Testing Of Advanced Composite Load Introduction Structure For Aircraft High Lift Devices." *25th ICAF Symposium – Rotterdam.* 27–29 May 2009

9. Bednarcyk B. A., Yarrington P. W., Collier C. S., Arnold S. M. "Progressive Failure Analysis of Composite Stiffened Panels."*47th AIAA/ASME/ASCE/AHS/ASC Structures, Structural Dynamics, and Materials Con.* AIAA 2006-1643, 1-4 May 2006

10. Lopez R. H., Luersen M. and de Cursi E. S. "Puck Failure Criterion As Constraint In The Optimization Of Laminated Composites." *WCCM8, ECCOMAS 2008, Venice, Italy*, June 30 – July 5, 2008

11. Krishnaraj V. "Effects of Drill Points on Glass Fibre Reinforced Plastic Composite While Drilling at High Spindle Speed." *Proceedings of the World Congress on Engineering 2008, London, U.K.* Vol II WCE 2008, July 2 - 4, 2008

12. Thompson R.B., "Nondestructive Evaluation and Life Assessment.", *ASM Handbook-Volume 11-Failure Analysis and Prevention*, 2002

13. MSC. Marc 2008 r1 Volume A: Theory and User Information

14. MSC. Marc 2008 r1 Volume B: Element Library

15. W.Weibull, Analysis of Fatigue Test Results. First Seminar on Fatigue and Fatigue Design, Columbia University, New York, pp. 68-69,1966.

16. R.B. Thompson, Nondestructive Evaluation and Life Assessment, ASM Handbook-Volume 11-Failure Analysis and Prevention,2002

17. R. Raišutis, E. Jasiūnienė, R. Šliteris, A. Vladišauskas, The review of non-destructive testing techniques suitable for inspection of the wind turbine blades, ISSN 1392-2114 ULTRAGARSAS (ULTRASOUND), Vol.63, No.1, 2008

18. Wong, B. S., Ow, W. Y. and Tui C. G., Non-destructive testing of fibre reinforced composites and honeycomb structures. Proceedings of Defence Materials and Mechanics Seminar 99, Singapore, 1999.

19. M.A. Drewry, G.A. Georgiou, A review of NDT techniques for wind turbines. The 45th Annual British Conference on NDT, Stratford-upon-Avon, UK, September 2006.